Chiang Mai J. Sci. 2024; 51(4): e2024059
https://doi.org/10.12982/CMJS.2024.059
Journal homepage : http://epg.science.cmu.ac.th/ejournal/

Research Article

Synthesis and Characterization of Red Pigment from Acid Regeneration Plant (ARP) By-product Via Rod Milling Process

Hai Song Woon [a]*, Keerthan Naidu [a], Lay Sheng Ewe [a], Lee Woen Ean [b,c] and Kean Pah Lim [d]

[a] Institute of Sustainable Energy (ISE), College of Engineering, Universiti Tenaga Nasional,43000 Kajang, Selangor, Malaysia

[b] Civil Engineering Department, College of Engineering, Universiti Tenaga Nasional, Jalan IKRAM-UNITEN, 43000, Kajang, Selangor, Malaysia

[c] Institute of Energy Infrastructure (IEI), Universiti Tenaga Nasional, Jalan IKRAM-UNITEN, 43000, Kajang, Selangor, Malaysia

[d] Physics Department, Faculty of Science, Universiti Putra Malaysia, 43400 Serdang, Selangor, Malaysia

*Author for correspondence; e-mail: hwoon@uniten.edu.my

Received: 8 August 2023
Revised: 10 January 2024
Accepted: 24 January 2024

ABSTRACT

Iron oxide waste from acid regeneration plants (ARP) is often discarded due to its non-profitability. This research aims to introduce a value-added process to convert iron oxide waste into red pigment via rod milling process. The iron oxide waste collected from ARP was grinded with a rod milling machine at 30 rpm for 24 hours. The ground product was then mixed with industrial-grade red pigment in various ratios. The mixed samples were then rod-milled again into ultra-fine particles. A total of seven samples were prepared, applied onto a canvas and analysed by energy dispersive X-ray spectroscopy (EDX) and X-ray diffraction (XRD) methods. From the analyses, the existence, composition, and orientation of iron oxide were established. The waste-derived red pigments were subsequently subjected to particle size analysis on a scanning electron microscopy (SEM) platform, with results showcasing the efficiency of the rod milling process. Colour-related properties of the samples before and after canvas application were investigated using the L*a*b* system with a chromameter. Empirical outcomes indicated that the a* value plays an important role in determining the redness of the sample. Overall, the a* values obtained were above 15 and gradually increased in accordance to the amount of industrial-grade red pigment added. The oil absorptivity of red pigments was also tested via an oil absorptivity test. Notably, the assay signified that particle size and porosity affect the amount of oil that can be absorbed by the pigment.

Keywords: acid regeneration plant (ARP), iron oxide, hematite, colour pigment material, rod-milling

1. INTRODUCTION

Steel is a common material utilised in many sectors across the globe. High-quality steel is characterised by surface smoothness. However, oxidation and scales rapidly form on the surface of steel once it has undergone the hot working process [1,2]. The eradication of scales, which could

range from 5 to 10 μm in thickness, is achievable by immersion in a pickle liquor that encompasses hydrochloric, nitric, and hydrofluoric acids [3,4]. Pickling is a continuous process; as debris and dirt from the steel accumulate in the acid, the pickle liquor gradually loses its efficiency. The pickling solution is deemed a 'spent acid' once its original acidic strength has been effectively reduced by 75 to 85% [7]. Nonetheless, even spent acids contain incredibly high acid levels, making it toxic to humans and the environment, and therefore require neutralisation alongside extremely cautious handling before disposal [5,6]. The spent acid may be sent to the acid regeneration plant (ARP) for treatment and recycling. Whilst the regenerated acid retrieved post-treatment can be reused for steel pickling, solid iron oxide wastes obtained as a by-product from the process are often discarded as previously, little value was found in investing in their further treatment.

Contrarily, iron oxide waste can be turned into fine particles via grinding, particles which might be useful for a wide range of applications due to its chemical stability [8,9,10]. In this study, a rod milling process is used to grind the iron oxide waste. Rod milling is capable of reducing the sample size by 0.1 μm to 2.0 μm [11]. One of the advantages of rod mill grinding is cost-effectiveness, as worn-out rods are cheap to replace [12]. Additionally, rod milling is more efficient than other grinding methods as it entails lower steel consumption compared to other mills [13,14,15]. The iron oxide waste is broken down into smaller fragments and transformed into pigments, varying in colour from red to dark red. The red pigment in particular exhibits excellent resistance to high temperatures, light, and unfavourable atmospheric conditions [9,10], thus making the prospect of its application attractive, specifically in terms of green technology [16,17].

This study aimed to transform iron oxide waste into a profitable material. The iron oxide waste constituents was identified using elemental analysis, whereas the effectiveness of the rod milling process was examined using particle size analysis. Colour analysis was subsequently performed to evaluate the colour properties of the waste-derived red pigment material. Finally, the oil absorptivity of the red pigments was tested via the Gardner-Coleman method [18,19].

2. MATERIALS AND METHODS

2.1 Materials

Iron oxide waste was collected from a local cold-rolling steel company (ARP). Initial inspection shows that the iron oxide waste is round pellet with 0.8 mm in diameter averagely. The colour of the waste appears to be dark grey as illustrated in Figure 1. The hardness of the iron oxide waste is estimated in between 4.5 Mohs to 5.5 Mohs.

2.2 Methods

The experimental procedure of this work can be summarized in the flowchart below (Figure 2).

The amount of raw material required for this study was approximately 200 grams. In the rod milling process, the ratio of steel rods to iron oxide waste was set at 6 to 1. Consequently, 1.2 kg of steel rods were used in this work. The iron

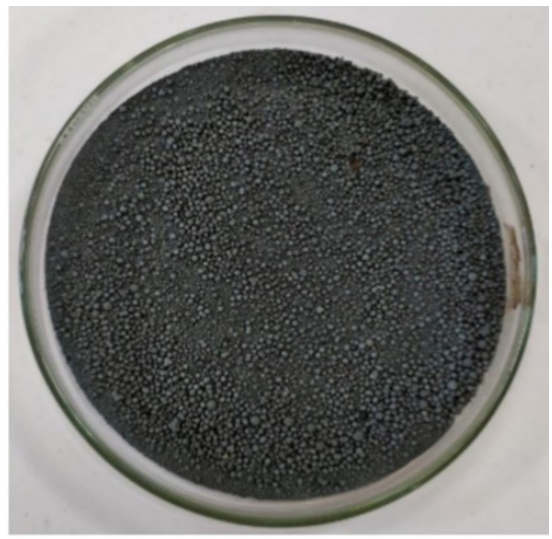

Figure 1. Iron oxide waste collected from ARP.

oxide waste was inserted into a drum together with the steel rods and operated, with the rod maintained at a rotational speed of 30 revolutions per minute. The duration of the grinding process was fixed at 24 hours.

The ground iron oxide waste product was mixed with industrial-grade red pigment (Brand: Amxess) at ratios shown in Table 1. To prepare samples for further analytical procedures, a binding medium (acrylic gel) was added to each before application onto a clean canvas. Samples were left to dry for a day.

The dominant element in the raw iron oxide waste was first analysed on an EDX machine. Next, the iron oxide waste was subjected to phase analysis by XRD, which revealed the sample crystal structure. The presence of hematite was determined through the 2 Theta values on the produced graph. SEM was employed to achieve a particulate view of the samples, whilst a chromameter (Minolta, Model CR10) [20] measured their colour properties in correspondence to the Colour Globe System (CIELAB system). The L*a*b* values [21] of a particular sample were derived from the readings of this device.

Finally, the red pigment was subjected to an oil absorptivity test, namely, the Gardner-Coleman method (ASTM D1483). Briefly, linseed oil was added dropwise to the pigment and slowly mixed to a paste of a set consistency. The quantity of oil required before the mixture became a paste was recorded as an indicator of the pigment's oil absorptivity [22].

3. Results and Discussion

The EDX analysis (Table 2) revealed that a majority of the iron oxide waste sample was composed of Fe (65.57%), followed by oxygen (23.17%) and carbon (8.06%). Notably, Si was the element with the lowest weightage of only 0.25%. In general, overall results showed that the purity of sample in terms of iron oxide content was more than 88%.

Chromameter-generated L*a*b* readings [11] before canvas application were tabulated in Table 3. These were essential in determining the

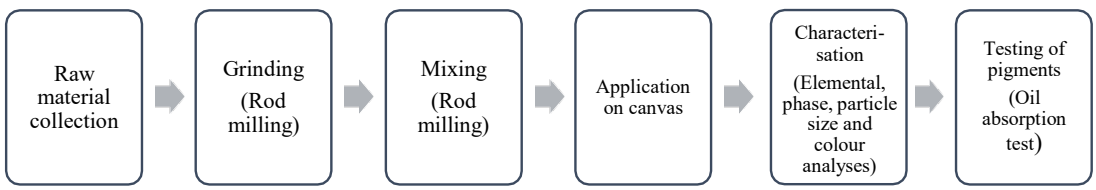

Figure 2. Flowchart of the experimental procedure.

Table 1. Sample names with mixing ratio.

Sample	Ratio (Pigment: Waste)
Sample 1	0:100
Sample 2	30:70
Sample 3	40:60
Sample 4	50:50
Sample 5	60:40
Sample 6	70:30
Sample 7	100:0

Table 2. Elemental analysis of iron oxide waste.

Element	Weight (%)
Carbon, C	8.06
Oxygen, O	23.17
Silicon, Si	0.25
Sulphur, S	0.95
Vanadium, V	0.51
Manganese, Mn	0.73
Iron, Fe	65.57
Nickel, Ni	0.76
TOTAL	100.00

Table 3. L*a*b* readings of samples before canvas application.

Sample	L*	a*	b*
Sample 1	36.6	+10.8	+5.0
Sample 2	36.3	+14.1	+8.9
Sample 3	36.7	+14.7	+9.5
Sample 4	36.9	+15.0	+9.8
Sample 5	36.9	+15.3	+9.9
Sample 6	37.0	+16.4	+10.9
Sample 7	38.7	+23.3	+14.6

colour properties of each of the seven samples. The L* value represents sample brightness, whereas a* denotes red for positive values and green for negative values. The negative value for b* signifies the colour blue and its positive value represents yellow [23]. The a* value is particularly crucial as it indicates sample 'redness' in this work.

Based on Table 3, the sample with the highest L* value was Sample 7 (38.7), whilst Sample 2 had the lowest value (36.3). The sample with the highest a* value (+23.3) was also Sample 7, presumably as it is an industrial-grade red pigment. Conversely, Sample 1 had the lowest a* value (+10.8), likely as it is primarily iron oxide waste. Sample 1 also expectedly recorded the lowest b* value (+5.0) against the high of Sample 7 (+14.6). The high values of a* (mostly greater than +14) in most samples revealed that the light reflected by the samples are between 620 nm to 750 nm in wavelength and thus indicated that visible red light is reflected.

The accompanying graph (Figure 3) showed the curve pattern of L* values (blue line) where there was an initial decline from Sample 1 to Sample 2 but progressed only upwards afterwards. The yellow line depicted b* values, which also exhibited a steady upward progression. Importantly, the graph demonstrated that a* values (red line) rose constantly as the sample tested became more heavily comprised of industrial-grade red pigments. Moreover, with the a* values that are greater than +14 implies that red light with wavelength between 620 nm to 750 nm is reflected by most of the samples in this work.

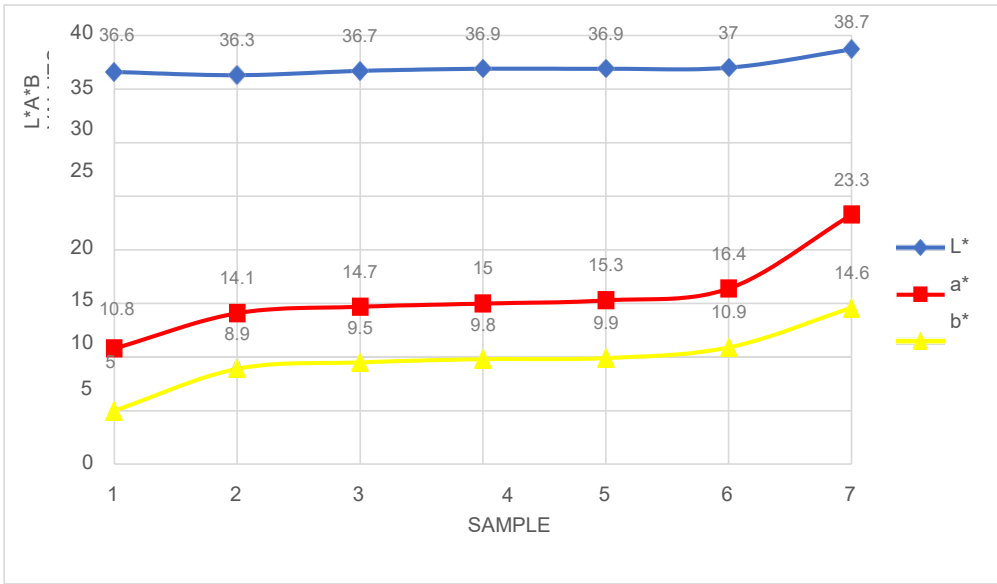

Figure 3. Graph of L*a*b* values (before application) against sample.

Table 4. L*a*b* readings of samples after application on canvas.

Sample	L*	a*	b*
Sample 1	29.7	+13.3	+6.2
Sample 2	33.2	+17.6	+12.1
Sample 3	33.4	+18.0	+12.4
Sample 4	34.2	+18.4	+12.7
Sample 5	34.6	+18.7	+12.9
Sample 6	35.0	+19.8	+13.4
Sample 7	35.8	+27.3	+17.3

Table 4 reveals that a* and b* readings were largely improved after the samples have been applied to and dried on the canvas. The samples were successfully dispersed by binding medium (acrylic gel) before applied onto the canvas. This can be observed that the a* values were increased by +3 in average although there was no significant change in the trend. Sample 7 had the highest L* value at 35.8, whereas Sample 1 was the lowest at 29.7. Sample 7 was also the sample with the highest a* value (+27.3) as opposed to Sample 1 which recorded the lowest (+13.3). Accordingly, Sample 1 accounted for the lowest b* value (+6.2), whereas Sample 7 had the highest (+17.3). The L* values decreased in general after applied and dried on the canvas. The dispersing followed by the drying process resulted a change in reflectivity and caused a decrease in the L* values.

The colour line trends produced by samples after their application onto the canvas are shown in Figure 4. The L* line (blue) was now missing the slight dip observed between Sample 1 and

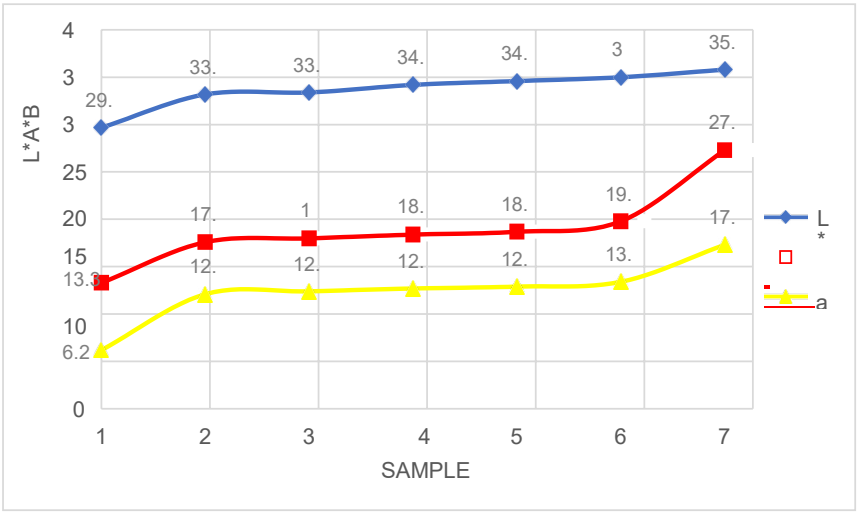

Figure 4. Graph of L*a*b* values (after application) against sample.

Sample 2 prior to canvas application, where it instead rose steadily all the way to Sample 7; which can be explained by the dispersive effect of the binding medium. This observation showcased the increasing brightness from Sample 1 to Sample 7. The b* values (yellow line) resulted in a similarly progressive upward curve pattern, representing the increasing yellowness from Sample 1 to Sample 7. Distinguishably, a* values increased with a progressive surge. Comparing Sample 1 and Sample 7 especially highlighted the drastic rise in redness as the ratio of industrial-grade red pigment became much greater.

The color property of the waste-derived red pigment after applied on canvas is illustrated in Figure 5.

Data from XRD analysis confirmed the presence of hematite (Fe_2O_3) in the samples (Figure 6). Plotting the samples together with that of standard diffraction pattern of hematite conclusively illustrated matching rhombohedral crystalline structures [24].

SEM was employed for particle size analysis on Sample 2, Sample 3, Sample 4, Sample 5, and Sample 6. The magnification used for these samples were 300x, 1000x, 2000x, and 5000x. Images of Sample 4 are presented (Figures. 7(a) to 7(d)). The size range of the particles found in the samples is listed in Table 4.

Overall, results (Table 5) showed that the diameter of a particle in all samples is less than 2 µm on average, a size suitable for use in building materials e.g. paint. Industrial-grade pigments were measured to be the smallest at 0.20 to 0.90 µm in range, whilst Sample 2 to Sample 6 displayed particulate sizes of 0.35 to 1.30 µm in diameter. Raw iron oxide waste (Sample 1) had the biggest particle size, with a range between 0.50 to 1.70 µm. Therefore, a longer milling period may be recommended in order to grind particles down to a diameter below 1 µm. Round particle shape in the samples suggested that the samples can easily be dispersed in the presence of binding medium (acrylic gel). Nevertheless, the rod milling process employed in this study was effective enough to mill samples down into sub-micron particles.

A final test undertaken was the oil absorptivity or Gardner-Coleman test. The assay involved the assessment of Sample 1, Sample 4, and Sample 7 for their oil-absorbing efficiency. Results are illustrated in Table 6.

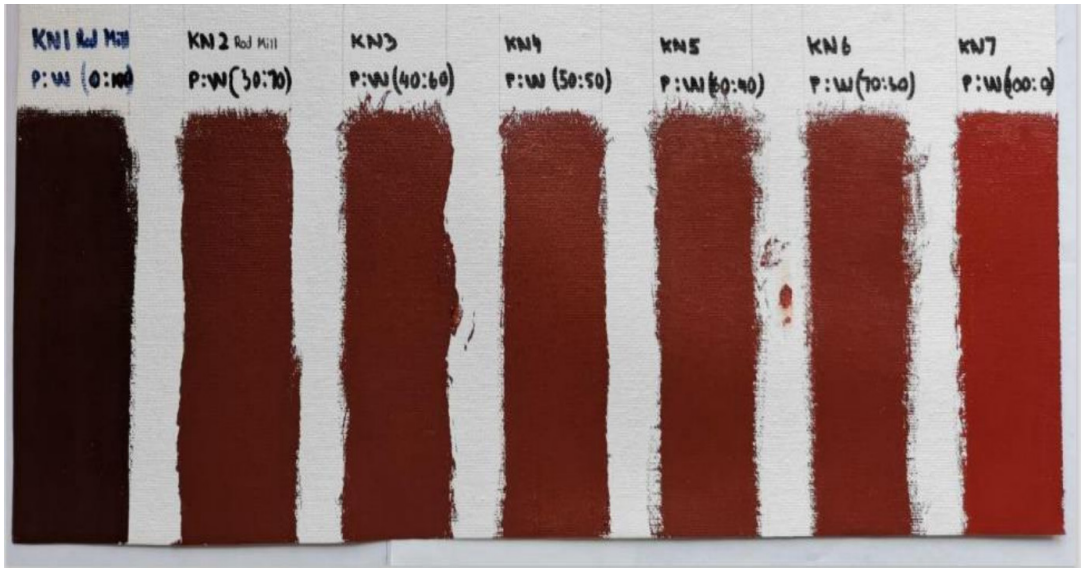

Figure 5. Waste-derived red pigment after application on canvas.

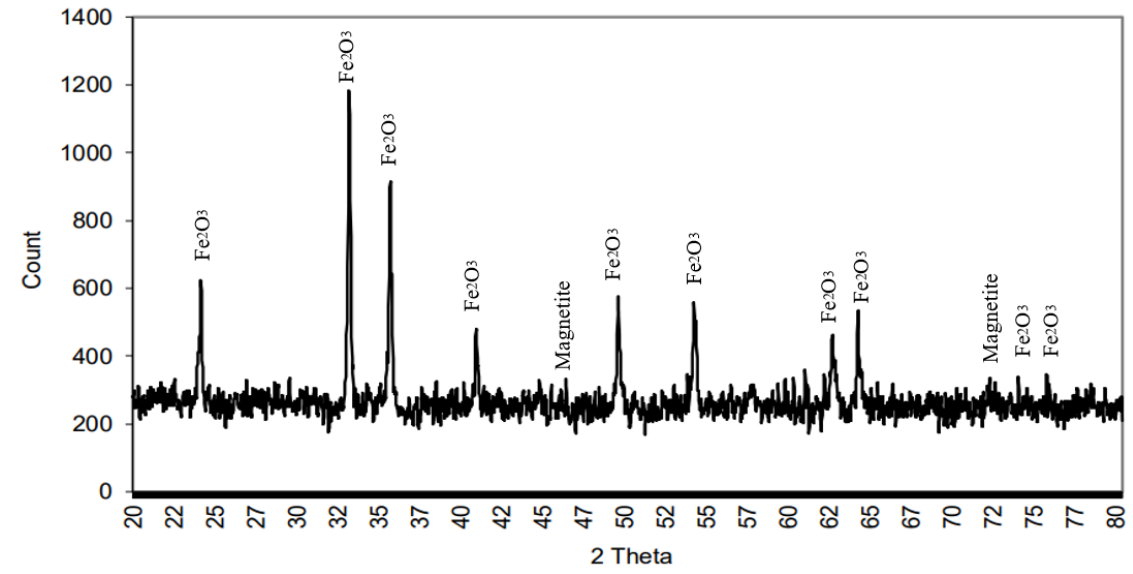

Figure 6. XRD pattern of sample 1.

The data implied that Sample 1 was an extremely poor oil absorber, generating an oil absorptivity value of only 6.19%. Within the industry, a colour pigment material is required to possess an oil absorptivity value of at least 20 %. Meanwhile, Sample 4 displayed a value of just above 20%, whilst Sample 7 or the industrial-grade pigment was the most absorbent at a value of 25.72%. Collectively, the absorptivity of Sample 7 coincided with its smaller particulate size, a

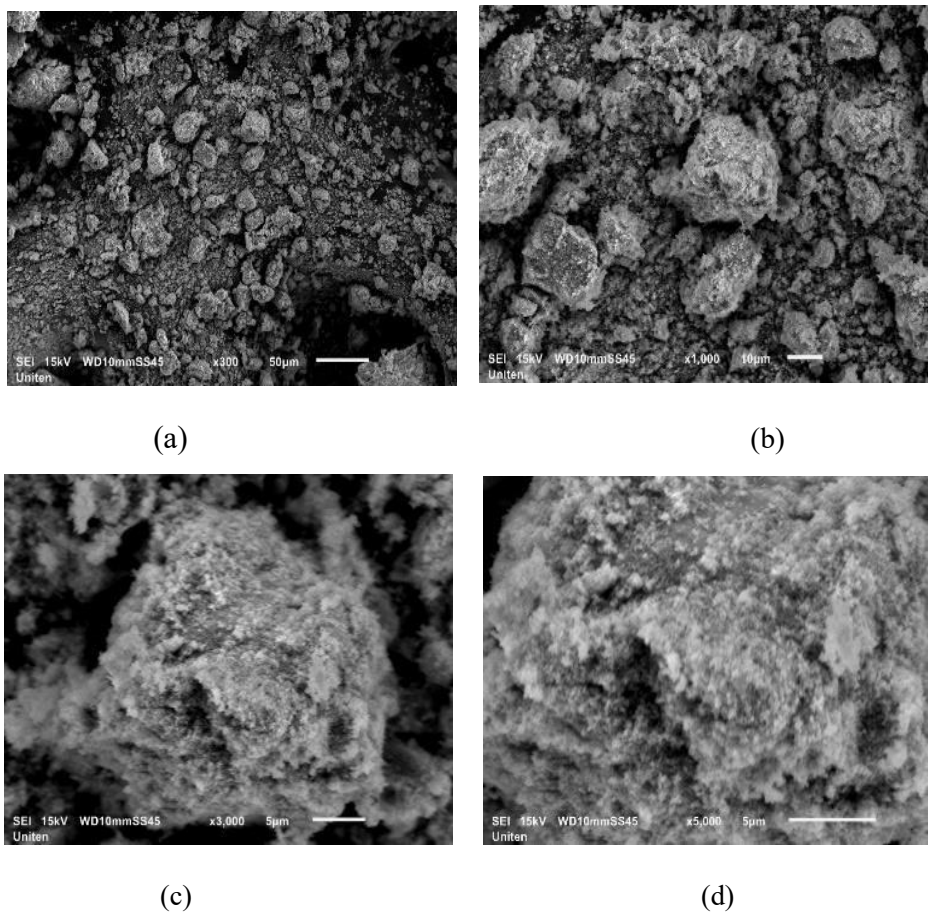

Figure 7. SEM images for sample 4 300X (a),1000X (b), 3000X (c) and 5000X (d) magnification.

Table 5. Range of sample particle size.

Sample Name	Range of Particle Size (µm)
Sample 1	0.50 – 1.70
Sample 2 – Sample 6	0.35 – 1.30
Sample 7	0.20 – 0.90

Table 6. Data of parameters involved in oil absorption test.

Sample	Mass of pigment, P (g)	Initial burette reading (mL)	Final burette reading (mL)	Oil Absorptivity, A (%)
Sample 1	18.02	40.5	41.7	6.19
Sample 4	18.03	40.5	44.4	20.12
Sample 7	18.08	44.6	49.6	25.72

characteristic which increases the total surface area of particle- to-oil contact. In conclusion, improving the surface area and particle size of a sample are crucial steps in achieving a higher oil absorptivity value.

4. Conclusions

In general, the rod milling process was effective in grinding iron oxide waste down into sub-micron particles. However, a longer milling period is essential to obtain particulate sizes of less than 1 μm. Additionally, results obtained from this work demonstrated the usability of iron oxide waste as a potential replacement material for current pigment sources in the building material production industry. The elemental and phase analyses revealed that iron oxide waste consisted mainly of hematite (Fe_2O_3) and small amounts of magnetite (Fe_3O_4). Scanning electron microscopy (SEM) then provided evidence that particle sizes were below 2 μm for most samples, and thus they may be used as a colour pigment in paint. Colour analysis was also instrumental in determining that a* values would experience an upward trend as more of the industrial-grade pigment material was added. Finally, oil absorptivity can be improved by increasing the milling period.

Acknowledgments

The author acknowledges College of Engineering, Universiti Tenaga Nasional for the equipment facility. This project is funded by UNITEN BOLD grant code J510050966.

Conflict of interest statement

The authors declare that there is no conflict of interest in this project.

References

[1] Rögener F., Lednova Y., Andrianova M. and Lednov A.V., *Bull. Nosov. Magnitogorsk. St. Tech. Univ.*, 2019; **17(2)**: 38-48. DOI 10.18503/1995-2732-2019-17-2-38-48.

[2] Deo B. and Boom R., *Fundamentals of Steel-making Metallurgy*, 7th Edn., Prantice Hall International, London, 1993.

[3] Woon H.S., Nicklaane K., Ewe L.S., Lim K.P., Ismail I. and Tan C.Y., *Proceedings of the 3rd International Sciences, Technology & Engineering Conference (ISTEC) 2018-Material Chemistry*, Penang, Malaysia, 17-18 April 2018; 020030. DOI 10.1063/1.5066986.

[4] Kumar S., *Material and Metallurgical Science*, 2nd Edn., Anuradha Agencies Educational Publishers, India, 2001.

[5] Schaffer J.P., Saxeba A., Antolovich S.D., Sanders Jr. T.H. and Warner S.B., *The Science and Design of Engineering Materials*, 2nd Edn., The McGraw-Hill International, Singapore, 1999.

[6] Arumugam M., *Materials Science*, Anuradha Agencies Educational Publishers, India, 2002.

[7] Regel-Rosocka M., *J. Hazard. Mater.*, 2010; **177**: 57-69.DOI 10.1016/j.jhazmat.2009.12.043.

[8] Quddus M., Rahman M.L., Khanam J., Biswas B., Sharmin N., Ahmed S., et al., *Int. Res. J. Pure Appl. Chem.*, 2018; **16(4)**: 1–9. DOI 10.9734/IRJPAC/2018/42935.

[9] Gerhard P., *ChemTexts*, 2022; **8**: 15. DOI 10.1007/s40828-022-00166-1.

[10] Gunter B. and Gerhard P., *Industrial Inorganic Pigments*, 3rd Edn., Wiley-VCH, London, 2005.

[11] Kapadia S., *Comminution in Mineral Processing*, MSc Thesis, Clausthal University of Technology, Germany 2018.

[12] Richardson J.F., Harker J.H. and Backhurst J.R., *Chem. Eng. J.*, 2002; **2**: 95-145.

[13] Schlanz J.W., *Mill Operators Symposium*, Spruce Pine, North Carolina, October 1987: 1-47.

[14] El-Eskandarany M.S., Aoki K. and Suzuki K., *J. Less-Common Met.*, 1990; **176(1)**: 113-118. DOI 10.1016/0022-5088(90)90295-U.

[15] Sherif M.E. and Ahmed H.A., *J. Alloy. Compd.*, 1995; **216(2)**: 213-220. DOI 10.1016/0925-8388(94)01282-M.

[16] Chen L., Zu X., Li D. and Wang X., *MATEC. Web Conf.*, 2016; **67**: 1-7. DOI 10.1051/matecconf/20166705024.

[17] Prim S.R., Folgueras M.V., Lima M.A. and Hotza D., *J. Hazard. Mater.*, 2011; **192(3)**: 1307–1313. DOI10.1016/j.jhazmat.2011.06.034.

[18] Janardhana R., Vijayakumar M., Mohan T. R.R. and Ramakrishnan P., *J. Eur. Ceram. Soc.*, 1996; **16(5)**: 567-54 DOI 10.1016/0955-2219(95)00165-4.

[19] Glancy C.W., Oil Absorption of Pigments; in Koleske J.V., ed., *Paint and Coating Testing Manual: 15th Edition of the Gardner-Sward Handbook*, ASTM International, USA, 2012: 300-310. DOI10.1520/MNL12209M.

[20] Minolta CR10 ; Available at: https://www.konicaminolta.eu/eu-en/hardware/measuring-instruments/colour-measurement/colour-readers/cr-10-plus.

[21] Ken P., What is CIELAB Color Space?; Available at: https://www.hunterlab.com/blog/what-is-cielab-color-space/#:~:text=CIELAB%20or%20CIE%20L*a,change%20humans%20see%20between%20colors.

[22] ASTM Standard, Standard Method for Oil Absorption of Pigment by Gardner-Coleman Method, D1483-95.

[23] Sanai A., Khottada W., Sirithip K. and Merat K., *Chiang Mai J. Sci.*, 2023; **50(4)**: e2023038. DOI 10.12982/CMJS.2023.038.

[24] Keerthan N., *Synthesis and Characterization of Red Pigment From Acid Regeneration Plant (ARP) By-Product Via Rod Milling Process*, Undergraduate Thesis, Universiti Tenaga Nasional, Malaysia, 2022.